

Research Article

The integration of GNSS RTK and IMU with extended particle filter

Duong Thanh Trung^{1*}

¹ Hanoi University of Mining and Geology; duongthanhtrung@humg.edu.vn

*Corresponding author: duongthanhtrung@humg.edu.vn; Tel.: +84–932202162

Received: 15 April 2024; Accepted: 14 June 2024; Published: 25 September 2024

Abstract: Global navigation satellite system is now widely applied for various applications. For high accuracy requirements such as surveying and mobile mapping system, real-time kinematic positioning (GNSS RTK) is commonly used. In the open sky, GNSS RTK can achieve centimeter level of accuracy in case of RTK fixed solution. However, in the GNSS-denied or -noisy environment such as under tree canopy or under bridge, GNSS RTK accuracy becomes worse. To overcome this issue, this study applies an integrated system consisting of an GNSS RTK module and Inertial Measurement Unit (IMU) to continuously provide navigation solutions including position, velocity, and attitude. For data fusion, Extended Particle Filter (EPF) is used in this research. EPF is considered as a hybrid estimation strategy to overcome the limitations of Extended Kalman Filter, that is popularly used in data fusion. The experimental results indicated the benefit of the integrated system, particularly in the GNSS hostile environment. In addition, the testing result illustrated that the performance of EPF is significant compared to that of EKF.

Keywords: GNSS RTK; IMU; Kalman Filter; Integration.

1. Introduction

Mobile Mapping System (MMS) has been widely applied for collecting geo-spatial data. In principle, MMS has two main steps: (1) capturing images by cameras or point clouds by laser scanners of objects of interest and (2) transforming them into mapping frames based on the internal and exterior orientation parameters [1, 2]. In the MMS, the position and orientation of the mapping sensors are popularly determined based on the integration of the Global Navigation Satellite System (GNSS) and Inertial Measurement Unit (IMU). Due to the low-cost and small size Micro-Electro-Mechanical System (MEMS) IMU is commonly used. However, the performance of the MEMS IMU is restricted, particularly in case of no additional constraint. [3] indicated that with the integration of GNSS and MEMS IMU in open sky areas such as highways and routes between countries, the position accuracy can reach the centimeter level. However, the position and attitude accuracy of MEMS IMU based in the downtown area where GNSS signals are often obstructed still do not meet the requirement of precise mapping with land-based MMS.

The main purpose of this study is thus to improve the performance of MMS utilizing GNSS/MEMS IMU integration while reducing their cost and size. Two kinds of error are presented in the error theory manner: systematic error and noise affecting the performance of the system. With MEMS IMUs, systematic errors are mainly from biases and scale factors of the gyroscopes and accelerometers. Calibration is implemented for treatment. However, intensive calibration with professional equipment would increase the cost significantly. In a practical sense, aid measurements from GNSS and other integrated sensors can compensate for the systematic error of the IMU. Developing an effective integration strategy is thus the

key to reducing the effect of systematic errors in an IMU. Although stable in the long term, GNSS measurements suffer from many sources of deterministic errors, such as ionosphere, troposphere delay, time synchronization error, and multipath [4]. For reliable aid measurements, GNSS data processing is considered.

Unlike systematic errors, noise is a form of un-deterministic error that can be treated by stochastic processing. For this task, the behavior of noise should first be modeled. The general theory about noise modeling was presented by [5] and the behavior of noise in an INS was described by [6, 7]. In general, the noise behavior in INS is divided into four types: white noise, random constant, random walk, and exponentially correlated random. Calibration is necessary and the noise is modeled by an appropriate mathematical process to understand the behavior of sensor noise. The Gauss-Markov process is popularly used to describe and model the behavior of noise. Given that the noise has been modeled, it is accounted for in the estimation process (i.e., Kalman filter (KF)) to obtain the highest probability of the output solutions.

The two effective ways to restrict these kinds of errors to improve the performance of the integrated navigation system are improving GNSS solution using GNSS Realtime Kinematic Positioning (RTK) and using optimal estimation algorithms. While GNSS RTK is easy to archive using enclosed commercial GNSS RTK receivers, this research focuses on estimation strategies. For estimation, the KF [8] is popularly known as an optimal estimation strategy. The KF aims to determine the state vector of the system states based on the minimization of covariance. The advantage of the KF is its reliability and simplicity. The main limitation of KF is that it can only be applied on linear function and assuming Gaussian noises. When the state and measurement model functions are non-linear, Linearized KF (LKF) or Extended KF (EKF) are applied instead of KF for estimation. In these strategies, non-linear functions are linearized keeping the first order of Taylor series expansion. The calculation sequence is similar to that of KF. However, LKF and EKF have limitations that were reported by several researchers [9–12]. The limitations of LKF or EKF are that only small errors are allowed during estimation and the presence of nonlinear error behavior might violate the assumption, thus generating biased solutions. Choosing an appropriate INS error model in KF-based systems is also not a trivial task [13].

One of the approaches to improve the performance of the integrated system is sampling-based filter approach such as Particle Filters (PF) [14, 15] and Unscented Kalman filter (UKF) [10, 13]. A typical and early developed algorithm of sampling-based filtering approaches is the PF. In the PF, the set of points (particles) is generated randomly with associated weights. The details of the PF were presented by [14, 16]. Besides the advantages that have been reported, PF also has several disadvantages that make it unpopular in integration. PF relies on important sampling, thus requires the design of a proposal distribution that can approximate the posterior distribution reasonably well. Designing such proposals is generally hard [14, 15]. Another improvement of sampling-based filter methods is using a hybrid scheme between generic PF and other linear Gaussian estimation methods. The study [17] introduced hybrid methods in which EKF and UKF Gaussian approximations are used as the proposal distribution for PF. The simulation result shows that this hybrid scheme, particularly PF based on UKF, performs better than other linear Gaussian estimation methods such as EKF and UKF. The study [18] applied and evaluated the performance of UPF, UKF, and EKF with INS/GPS integration using MEMS IMU. The results indicate that the improvement of non-linear, non-Gaussian estimation compared with EKF was about 10% to 20%. The study [19] evaluated the feasibility of some estimations for non-linear function in positioning. The study [20] evaluated the performance of a low-cost INS/GPS integration system using the street return algorithm.

In general, the advantage of sampling-based methods over KF-based methods is that it can be applied on a non-linear function with arbitrary density distribution. Their performance

is thus better than that of KF-based methods. Some limitations of sampling-based methods were still reported. The choice of an optimal proposal probability density function to draw samples is difficult to implement. The manner of generating the samples is also a difficult task for certain applications. Computational burden is the main disadvantage of these algorithms for real-time applications. In order to deal with non-Gaussian noise in the GNSS/IMU system, this study applies a non-linear, non-Gaussian estimation algorithm, called Extended Particle Filter (EPF) to improve the performance of the system.

2. Methods

2.1. Integration strategy

In the integration scheme, the GNSS carrier-phase measurements are processed using a base station. The GNSS RTK module provides positions and velocities in the navigation frame as the updating measurements for the data fusion engine such as EKF. Angular rates and specific forces, the output of IMU is processed based on an INS mechanization to provide position, velocity, and attitude. In data fusion engine, EKF is first applied. A set of particles is generated based on Gaussian approximation from EKF output. EPF is then applied to provide optimal solutions. Figure 1 shows the integration scheme.

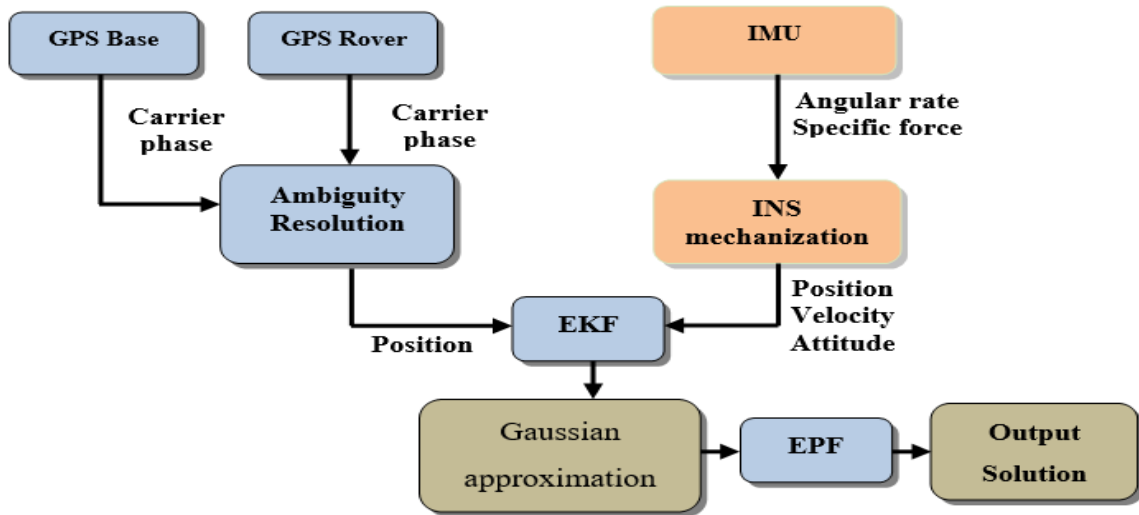


Figure 1. The integration scheme.

2.2. Extended Kalman Filter

EKF is the combination of nonlinear and linearized filtering techniques. In the prediction step, the nonlinear function is directly used to time-update the state vector, but the associated covariance is estimated based on the Jacobian matrix:

$$x_k = f(x_{k-1}) + w_{k-1} \tag{1}$$

where x_k is the state vector consisting of position, velocity, and attitude at time k ; w is system noise. Components of state vector is described in the below equation:

$$x_{21 \times 1} = [r^n v^n r_b^n b_g b_a s_g s_a]^T \tag{2}$$

where r^n , v^n , and r_b^n are position, velocity, and attitude of the system in the navigation frame; b_g , b_a , s_g , and s_a are the biases and scale factors of the IMU, respectively.

In the measurement update step, state vector is propagated through the nonlinear measurement equation to calculate the innovation in the next step:

$$z_k = h(x_k) + n \tag{3}$$

where z_k is an updating measurement; $h(x_k)$ is a function of a state vector; n is the measurement noise.

Figure 2 depicts the process and the performance of the EKF.

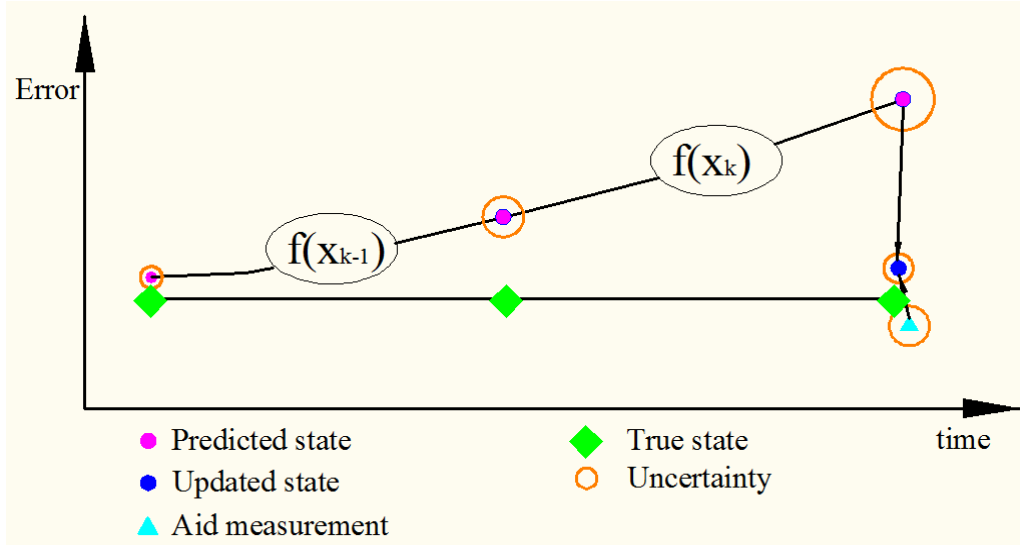


Figure 2. The process and performance of the EKF.

2.3. Estimation with Extended Particle filter

Generally, the hybrid estimation strategies use a Gaussian approximation as the proposal distribution to generate particles. A Gaussian approximation of $P(x_k | x_{k-1}, z_{0:k})$ using EKF is called Extended Particle Filter (EPF). In these strategies, first, EKF is implemented to obtain the Gaussian approximation of $P(x_k | x_{k-1}, z_{0:k})$ including estimates of the state and their covariances. Then the particles are sampled based on those estimates.

$$\hat{x}_k^i = f(x_{k-1}^i, w^i) \tag{4}$$

With associated weight

$$w_k^i = \frac{p(z_k | \hat{x}_k^i) p(\hat{x}_k^i | x_{k-1}^i)}{N(\hat{x}_k, P_k)} \tag{5}$$

where $P(x_k | x_{k-1}, z_{1:k-1})$ denotes the distribution density function of x_k given x_{k-1} and $z_{1:k-1}$; $N(\cdot)$ denotes the Gaussian distribution; \hat{x}_k, P_k are mean and covariance approximated by EKF.

The state vector and covariance matrix of the current time epoch are determined by weighted average of the generated particle:

$$\hat{x}_k^- = \sum_{i=0}^N w^i x_k^i \tag{6}$$

$$P_{xx}^- = \sum_{i=0}^N w^i (x_k^i - \hat{x}_k^-) (x_k^i - \hat{x}_k^-)^T \tag{7}$$

Figure 3 describes the flowchart of the hybrid estimation and Figure 4 illustrates the principle of this estimation strategy.

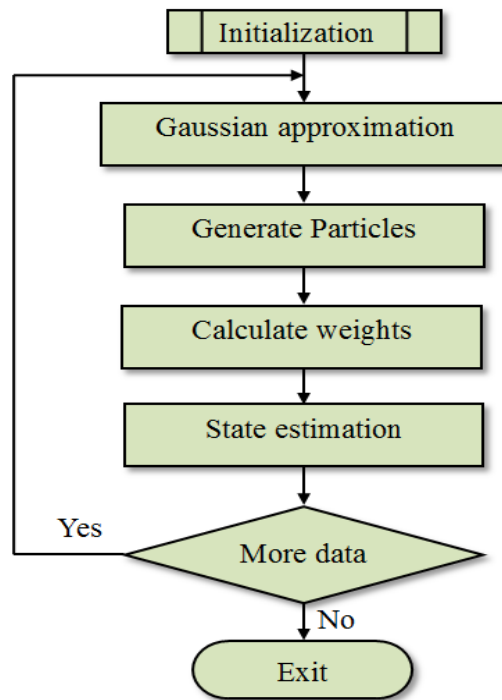


Figure 3. Flowchart of Extended Particle Filter.

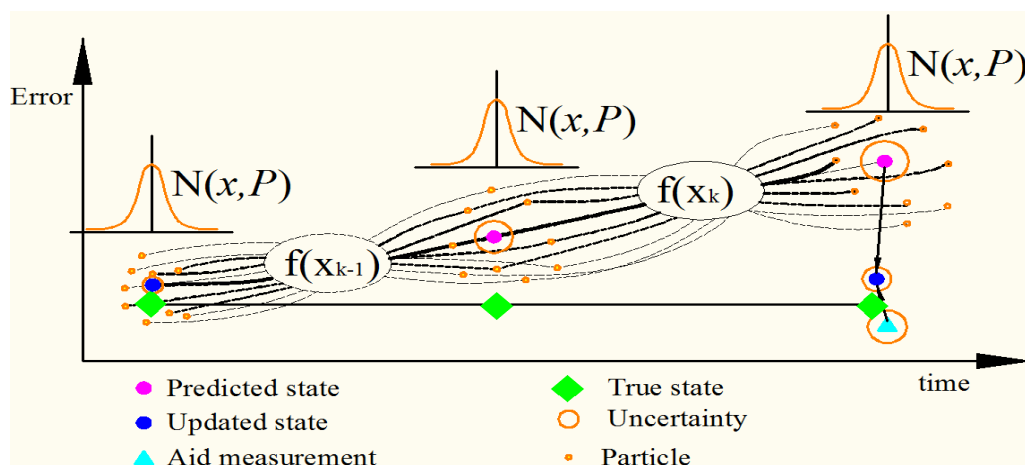


Figure 4. Principle of Extended Particle Filter with Gaussian approximation.

3. Experiment and discussion

The purpose of the experiment is to evaluate the performance of the integrated system in comparison with a stand-alone GNSS receiver and between estimation strategies, including EKF and EPF. For those purposes, three systems were set up on a platform to evaluate the performance of the given system and methodology. The reference system is a dual frequency RTK GNSS receiver, Leica viva GS16. The system is connected with the VNGEONET CORSs for RTK fixed solutions. In addition, various check points were built along the reference trajectory. The coordinates of the check points were determined by using a total station, the accuracy is guaranteed at the level of centimeter. The first testing system is a single frequency GNSS receiver, GNSS EVK-NEO M8T to provide Single Point Positioning (SSP) solution. The second testing system is the integration of the GNSS RTK module, Ublox ZED-F9P and an IMU, Xsens-MTi-3. Specification of the integrated system is described in table 1. The integrated system and testing platform is depicted in Figures 5a, 5b.

Table 1. The specification of main components.

Devices	Unit	Value
Number of concurrent GNSS	GNSS system	4
Position accuracy	m	0.01 m + 1 ppm
Output rate	Hz	1 Hz
Gyroscope	Unit	Value
In-run Bias	[°/s]	10
Noise density	[°/s/√Hz]	0.007
Non-linearity	[%FS]	0.1
Accelerometer		
In-run Bias	[mg]	0.03
Noise density	[mg/√Hz]	120
Non-linearity	[%FS]	0.5

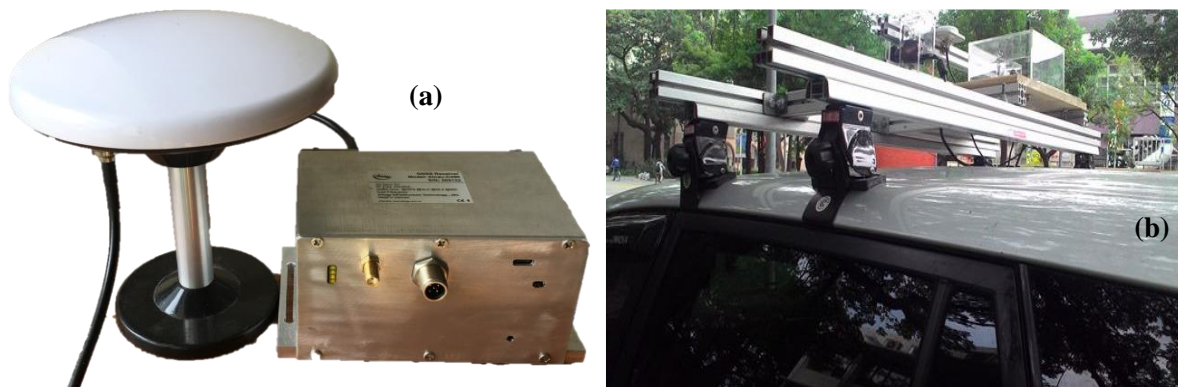


Figure 5. The integrated system (a) and testing platform (b).

The data were collected continuously under different environment scenarios, including in open sky view and GNSS-denied view in Hanoi, Vietnam (Figure 6). The integrated GNSS RTK/IMU data is processed by a software module written in C++ programming language with two algorithms, EKF and EPF. The graphical user interface of the software module can be seen in Figure 7a. For analysis, four output solutions including GNSS SSP, GNSS RTK, GNSS RTK/IMU with EKF and GNSS RTK with EPF are compared with GPS time synchronization. The trajectory of the test can be seen in Figure 7b. For detailed analysis, enlargements of two typical testing scenarios including in the open sky view and under bridge view as shown in Figures 8a, 8b. The numerical analysis can be seen in Tables 2, 3.



Figure 6. Testing scenarios in open sky view (a) and GNSS-denied view (b).

Table 2. Numerical results in the open sky view area.

	Availability (%)	Min(m)	Max(m)	Mean(m)	Std. Deviation(m)
GNSS SSP	99	0.450	9.610	2.400	1.560
GNSS RTK	95	0.002	0.720	0.030	0.026
GNSS RTK/IMU EKF	99	0.003	0.810	0.040	0.035
GNSS RTK/IMU EPF	99	0.003	0.710	0.040	0.032

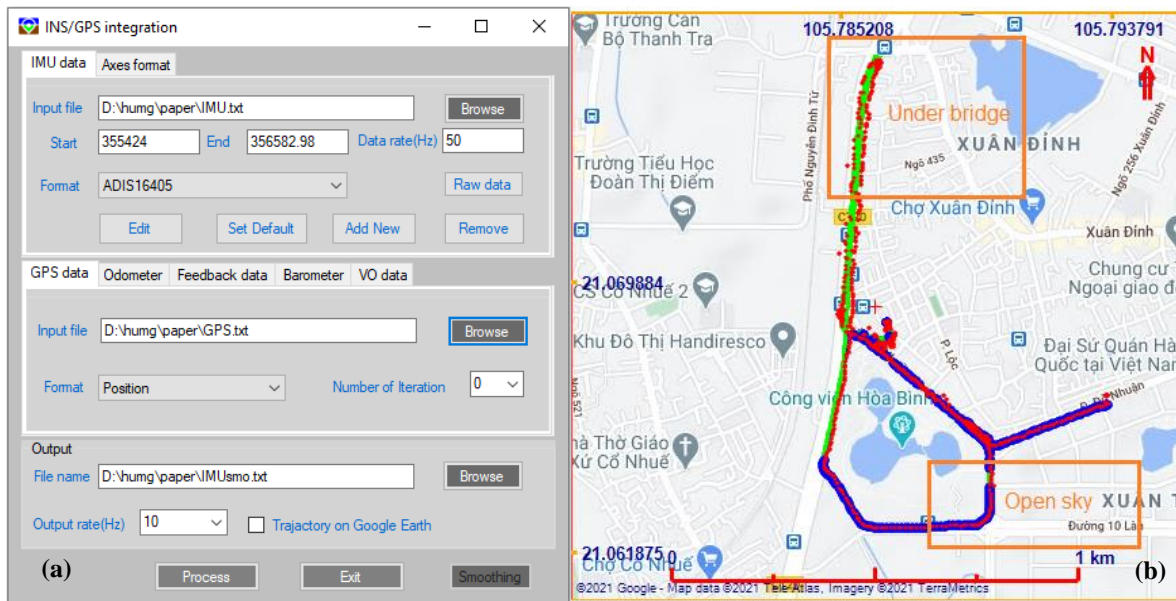


Figure 7. (a) GUI of the software module, (b) Testing trajectory of the test.

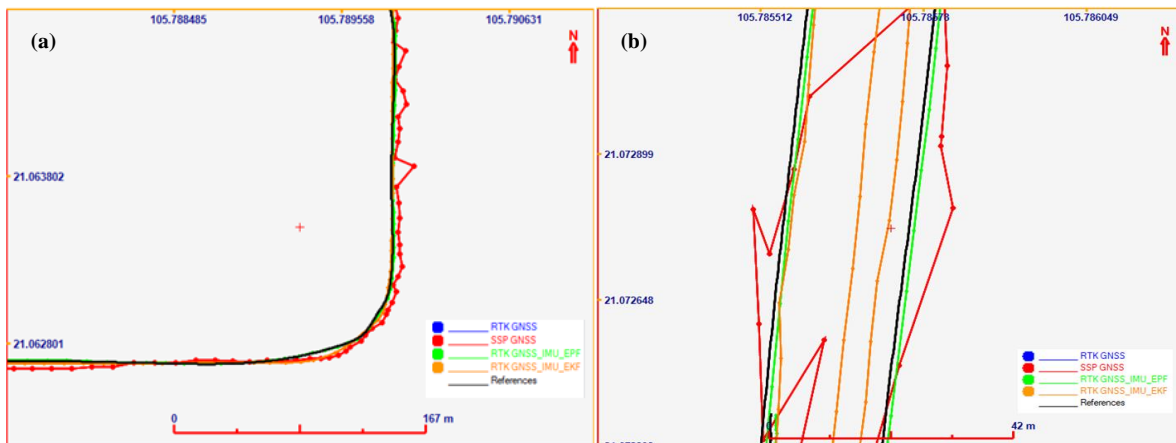


Figure 8. (a) Enlargement of scenario open sky view area in the test, (b) Enlargement of under bridge area in the test.

Table 3. Numerical result in the under-bridge area.

	Availability (%)	Min(m)	Max(m)	Mean(m)	Std. Deviation(m)
GNSS SSP	72	0.120	20.600	4.650	5.560
GNSS RTK	57				
- SSP	20	0.05	5.820	3.540	4.563
- RTK float	0				
- RTK fixed	0				
GNSS RTK/IMU_EKF	99	0.015	10.530	2.401	3.403
GNSS RTK/IMU EPF	99	0.012	1.530	1.240	1.340

From the test, in the open sky, GNSS can continuously provide solutions with homogenous accuracy. GNSS RTK can provide a position at accuracy about 3 centimeters while GNSS SSP can provide 1.5-meter level of accuracy. Consequently, the integration of GNSS RTK/IMU with EKF or EPF can provide navigation solution at accuracy of about 3-4 centimeters. In this case EKF or EPF do not help to improve the accuracy of the system because the position update mainly relies on the GNSS RTK.

In the under-bridge environment, accuracy, and availability of GNSS degrade seriously. The availability of GNSS SPP solution is 72% at accuracy of about 6 meters. In this testing scenario, GNSS RTK cannot provide RTK fixed solution any time, only RTK float solution

of 20% and 57% of SSP. Overall positional standard deviation of GNSS RTK is about 5 meters. In contrast, with the integration of GNSS RTK and IMU, availability of navigation solution is still at 99%. In this case, the performance of EPF is better than that of EKF with standard deviation of 1.3m compared to 3.4m in the EKF.

4. Conclusions

This research evaluates the performance of an integration scheme that combines the GNSS RTK and IMU and an estimation strategy called EPF.

Field test in different environmental scenarios were implemented to collect data for analyzing the performance of the different integration architecture and estimation strategies.

The result from the experiment indicated that the integration of GNSS RTK/IMU enables to seamlessly provide navigation solution in any environmental scenarios. However, the positional accuracy of the system mainly relies on the position provided by GNSS.

The EPF with non-Gaussian noise estimation performs a significant improvement in terms of positional accuracy compared to that of EKF.

Author contribution statement: Designed the study conception: D.T.T.; collected data: D.T.T.; developed the theoretical research: D.T.T.; processed the data and performed the simulations: D.T.T.; analyzed the data: D.T.T.; contributed largely to revising the final manuscript: D.T.T.

Acknowledgments: This study is supported by project No. ĐT.CNKK.QG.011/23 funded by Ministry of Industry and Trade of the Socialist Republic of Vietnam.

Competing interest statement: The authors declare no conflict of interest.

References

1. Toth, C.K. R&D of mobile LIDAR mapping and future trends. Proceedings of SPRS, Baltimore, Maryland, 9–13 March 2009.
2. Rau, J.Y.; Habib, A.F.; Kersting, A.P.; Chiang, K.W.; Bang, K.I.; Tseng, Y.H.; Li, Y.H. Direct Sensor Orientation of a Land-Based Mobile Mapping System. *Sensors* **2011**, *11*, 7243–7261.
3. Huang, Y.W.; Chiang, K.W. The Applicability analysis of LC and TC low cost MEMS IMU/GPS POS systems for land based MMS. Proceeding of the ENC-GNSS, 2009.
4. Seeber, G. Satellite geodesy. Walter de Gruyter, Berlin, New York, 2003.
5. Shin, E.H. A quaternion-based unscented Kalman filter for the integration of GPS and MEMS INS. Proceedings of ION GNSS, Long Beach, California, 21–24 September 2004.
6. Titterton, D.H.; Weston, J.L. Strapdown inertial navigation technology, second edition. American Institute of Aeronautics and Astronautics, Reston, USA, 2004.
7. Rogers, R.M. Applied mathematics in integrated navigation systems. Third Edition, AIAA, Virginia, USA, 2007.
8. Kalman, R.E. A new research approach to linear filtering and prediction problem. *J. Basic Eng.* **1960**, *82*, 35–45.
9. Brown, R.G.; Hwang, P.Y.C. Introduction to random signals and applied Kalman filtering. John Wiley & Sons Inc., 1997.
10. Julier, S.J.; Uhlmann, J.K. New extension of the Kalman filter to nonlinear systems. Proceedings of the SPIE, 1997, pp. 182–193.
11. Chiang, K.W.; Noureldin, A.; El-Sheimy, N. Multi-sensors integration using neuron computing for land vehicle navigation. *GPS Solutions* **2003**, *6*(3), 209–218.

12. El-Sheimy, N.; Abdel-Hamid, W.; Lachapelle, G. An adaptive neuro-fuzzy model for bridging GPS outages in MEMS-IMU/GPS land vehicle navigation. Proceedings of ION GNSS, Long Beach, California, 21–24 September 2004.
13. Shin, E.H. Estimation techniques for low-cost inertial navigation. UCGE Reports Number 20156, 2005.
14. Gordon, N.J.; Salmond, D.J.; Smith, A.F.M. Novel approach to nonlinear/non-Gaussian Bayesian state estimation. *IEE Proceedings F (Radar Signal Processing)* **1993**, *140(2)*, 107–113.
15. Haug, A.J. A tutorial on Bayesian estimation and tracking techniques applicable to nonlinear and non-gaussian processes. MITRE technical report, 2005.
16. Lee, J.K. The estimation method for an Integrated INS/GPS UXO geolocation system. Technical Report No. 493, The Ohio State University, Columbus, Ohio, 2009.
17. Van Der Merwe, R.; Doucet, A.; De Freitas, N.; Wan, E. The unscented particle filter. *Adv. Neural Inf. Process. Syst.* **2000**, 584–590.
18. Duong, T.T.; Chiang, K.W. Non-linear, non-Gaussian estimation for INS/GPS integration. *Sensor Letter* **2012**, *10(6)*, 1081–1086.
19. Dung, P.T.; Trung, D.T. Ability of filtering algorithms for non-linear model used for positioning. *J. Min. Earth Sci.* **2017**, *58(4)*, 34–42.
20. Thang, N.V.; Thang, P.M.; Tan, T.D. The performance improvement of a low cost INS/GPS integration system using the street return algorithm. *VN J. Mech.* **2012**, *34(4)*, 271–280.